

# Synthesis of heteroarm star copolymers by anionic copolymerization of binary macromonomers

Koji Ishizu\* and Kazuo Kuwahara

Department of Polymer Science, Tokyo Institute of Technology, 2-12 Ookayama, Meguro-ku, Tokyo 152, Japan

(Received 7 March 1994)

Vinylbenzyl-terminated polystyrene (PS) and polyisoprene (PI) macromonomers were synthesized by the coupling reaction of corresponding living anions with *p*-chloromethylstyrene. Anionic copolymerizations of binary PS and PI macromonomers were carried out in benzene with *n*-butyllithium as an initiator. The reactivity ratios of these systems were close to an azeotropic copolymerization. We studied the microphase separation of  $A_nB_n$  star-like (comb-shaped) copolymers by electron microscopy.  $A_nB_n$  star copolymers formed clear microphase-separated structures and their domain sizes were smaller than those of corresponding diblock copolymers.

(Keywords: macromonomer; star copolymer; microphase separation)

## INTRODUCTION

The particular chemical structure of block copolymers is reflected in the most fundamental and interesting ways by incompatibility effects. Leibler<sup>1</sup> was the first to make clear theoretically the order-disorder transition of diblock copolymers. Subsequently, de la Cruz and Sanchez<sup>2</sup> calculated, from mean-field theory, the phase stability criteria and static structure factors for a simple AB graft copolymer, for star copolymers with equal numbers of A and B arms ( $A_nB_n$  star: heteroarm star), and for *n*-arm star diblock copolymers. They predicted that it is easier to phase-separate star copolymers than the corresponding graft and block copolymers.

There have been reports<sup>3-10</sup> of attempts to prepare  $A_nB_n$  star copolymers. Berlinova and Panayotov<sup>3</sup> prepared amphiphilic diblock macromonomers possessing a central unsaturated group. In the radical *cis-trans* isomerization of these diblock macromonomers, four- to eight-arm amphiphilic  $A_nB_n$  star copolymers were formed. Rempp and co-workers<sup>4,5</sup> prepared  $A_nB_n$  star copolymers by using a three-step anionic process. A living precursor polymer was made first; this was used to initiate the polymerization of a small amount of bis-unsaturated monomer, so as to build star molecules. Each of the resulting cores was linked to the precursor chains that had contributed to its initiation. This living star polymer was subsequently used to initiate the polymerization of another monomer, implying that new branches were growing out from the core. However, it does not seem that the initiation step from a living star polymer is as rapid as the propagation step, owing to high segment density around the core anions. More recently, Kanaoka *et al.*<sup>11</sup> have shown that a similar synthesis of amphiphilic  $A_nB_n$  star copolymers is possible via living cationic polymerization. The hydrogen iodide/Lewis acid initiating

system induces living cationic polymerization of not only alkyl vinyl ethers but also those having a pendent ester group that leads to water-soluble polymers.

We have suggested a novel architecture for  $A_nB_n$  star copolymers by means of the organized polymerization of a microphase-separated structure formed by diblock macromonomers possessing central polymerizable groups. In this environment, the polymerizable groups at the position of the block junction should be oriented regularly at the domain interfaces. The interface is narrow (~2–5 nm) for block copolymers possessing narrow molecular weight distributions, regardless of molecular weight<sup>12-15</sup>. We have reported the synthesis of  $A_nB_n$  star copolymers by means of organized polymerization of diblock macromonomers possessing central polymerizable groups<sup>16,17</sup>. Microphase-separated film of diblock macromonomer, possessing central vinylbenzyl groups, was obtained in the presence of photosensitizer and crosslinker by the casting method. Microgelation of the central vinylbenzyl groups with crosslinker led to the formation of  $A_nB_n$  star copolymer under u.v. irradiation. These star copolymers were also obtained by addition-condensation of diblock copolymer film possessing central isoprene groups<sup>18</sup>.

Next, we suggest another architecture of  $A_nB_n$  star-like copolymers by means of copolymerization of A and B binary macromonomers. It is well known that free-radical copolymerization of styrene and maleimide forms an alternating copolymer. It is therefore interesting to study the free-radical copolymerization behaviour of vinylbenzyl- and maleimide-terminated binary macromonomers. However, we have not yet succeeded in synthesizing such maleimide-terminated macromonomers under the present conditions. If the vinylbenzyl-terminated macromonomers have the same polymerization reactivity, regardless of the chemical species of the macromonomer segments and of their molecular weights, the composition

\* To whom correspondence should be addressed

of  $A_nB_n$  star-like (comb-shaped) copolymers formed may be controlled by the feed molar ratio of A and B binary macromonomers.

This article reports the preparation of vinylbenzyl-terminated polystyrene (PS) and polyisoprene (PI) macromonomers by the coupling reaction of corresponding living anion ends with *p*-chloromethylstyrene (CMS). Anionic copolymerization of binary PS and PI macromonomers was carried out in benzene, and copolymerization reactivity was estimated from the distribution functions by gel permeation chromatography (g.p.c.) of the comb-shaped copolymers produced. We also studied the microphase separation of  $A_nB_n$  star copolymers.

## EXPERIMENTAL

### Synthesis and characterization of macromonomers

Vinylbenzyl-terminated PS macromonomers were synthesized by the coupling reaction of poly(styryllithium) living anion with an excess amount of CMS in a benzene-tetrahydrofuran (THF) mixed solvent<sup>19,20</sup>. Styrene and CMS (from Seimi Chemical Ind. Ltd) monomers were dried over a mixture of calcium hydride-lithium aluminium hydride and then distilled under vacuum. Subsequently, styrene was purified with triphenylmethyl sodium in vacuum. Benzene was dried over sodium metal and then purified with *n*-butyl lithium (*n*-BuLi) under vacuum. THF was distilled from its solution of  $\alpha$ -methylstyrene (MS) tetramer sodium anion under vacuum. Vinylbenzyl-terminated PI macromonomers were also synthesized by the coupling reaction between poly(isoprenium lithium) end-capped with MS and CMS in a benzene-THF mixture<sup>20</sup>. Both products were purified three times by reprecipitation from benzene solution with methanol.

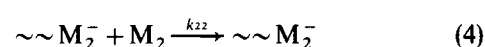
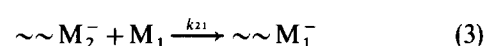
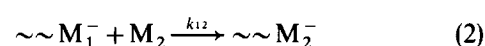
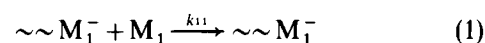
The number-average molecular weight ( $\bar{M}_n$ ) of PS macromonomers was determined by g.p.c. (Tosoh high-speed liquid chromatograph HLC-8020) with THF as eluent at 38°C, a TSK gel GMH<sub>XL</sub> column and a flow rate of 1.0 ml min<sup>-1</sup> using a calibration curve of standard PS samples. The  $\bar{M}_n$  of PI macromonomers was determined by vapour pressure osmometry on a Corona NA 117 vapour pressure osmometer in benzene. The polydispersity ( $\bar{M}_w/\bar{M}_n$ ) was determined from g.p.c. distribution functions improved by the reshaping method<sup>21</sup> with a personal computer. The content of terminal vinylbenzyl groups was determined by the area ratio of refractive index (r.i.) and u.v. (292 nm) intensities on a g.p.c. chart (by a calibration curve constructed from a mixture of PS or PI and *p*-methylstyrene)<sup>20</sup>. The characteristics of PS and PI macromonomers used are listed in Tables 1 and 2, respectively.

### Anionic copolymerization of binary macromonomers

Anionic copolymerization of binary macromonomers was carried out in benzene at 25°C using *n*-BuLi as initiator in a sealed glass apparatus under a pressure of 10<sup>-6</sup> mmHg. In this copolymerization process, the initiator solution was dropped instantaneously into the solution of binary macromonomers, because it was impossible to remove the impurity (a small amount of water) from the benzene solution of macromonomers. After polymerization, the copolymerization solution was poured into a large excess of methanol.

Anionic copolymerization of binary macromonomers will form the structure of comb-shaped copolymers. Although the primary structure is the comb-shaped

copolymer type, its solution and solid properties will be similar to those of heteroarm star block copolymers. In the preparation process, the relevant copolymerization parameters are very important in determining the arm distribution in the resulting comb-shaped copolymers, regardless of the same terminal end (vinylbenzyl group) of the macromonomers. Generally, anionic species are composed of three types: ion pair, solvent-separated ion pair and free ion. The terminal ion pairs do not dissociate into the respective free ions in hydrocarbon solvents, such as benzene, used in this work. Therefore, kinetic equations are expressed with four propagation steps, as developed by Mayo and Lewis<sup>22</sup>. Two monomers  $M_1$  and  $M_2$  are defined as the vinylbenzyl-terminated PS and PI macromonomers, respectively. The kinetic equations, (1)–(4), are shown with the corresponding rate expression for loss of monomer:



Each propagation reaction has a characteristic rate constant  $k_{ab}$ , where the first subscript refers to the active centre and the second subscript refers to the monomer. Defining the propagation rate constant ratios  $k_{11}/k_{12}$  and  $k_{22}/k_{21}$  as  $r_1$  and  $r_2$ , respectively, one finally obtains:

$$\frac{d[M_1]}{d[M_2]} = \frac{[M_1] r_1 [M_1] + [M_2]}{[M_2] r_2 [M_2] + [M_1]} \quad (5)$$

The reactivity ratios  $r_1$  and  $r_2$  can be estimated by the method of Fineman and Ross<sup>23</sup>. The conversion was controlled at less than 25 wt% in order to estimate the copolymerization reactivities. The mole fraction of the monomer  $M_1$  in the copolymer ( $f_1$ ) was determined by the area ratio of the r.i. and u.v. (252 nm) intensities on a g.p.c. chart (using a calibration curve constructed from a mixture of PS and PI homopolymers: Figure 1).

In order to study the microphase separation of

Table 1 Characteristics of PS macromonomers

Code	$\bar{M}_n^a \times 10^{-4}$	$\bar{M}_w/\bar{M}_n^a$	Vinylbenzyl group <sup>b</sup> (number/1-polymer)
SM1	1.29	1.23	1.02
SM2	2.93	1.36	1.06
SM3	4.20	1.32	0.82

<sup>a</sup> Determined by g.p.c.

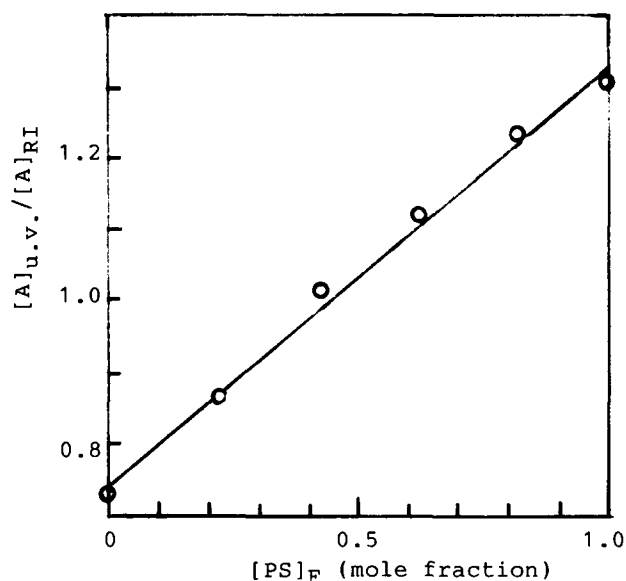
<sup>b</sup> Determined by g.p.c. with r.i. and u.v. double detectors

Table 2 Characteristics of PI macromonomers

Code	$\bar{M}_n^a \times 10^{-4}$	$\bar{M}_w/\bar{M}_n^a$	Vinylbenzyl group <sup>b</sup> (number/1-polymer)
IM1	1.93	1.13	0.80
IM2	1.95	1.01	1.04

<sup>a</sup> Determined by g.p.c.

<sup>b</sup> Determined by g.p.c. with r.i. and u.v. double detectors



**Figure 1** Calibration curve constructed from a mixture of PS and PI homopolymers by using g.p.c. double detectors (r.i. and u.v. at 254 nm). [A]<sub>u.v.</sub>, area of g.p.c. distribution of PS homopolymer in u.v. monitor; [A]<sub>RI</sub>, area of g.p.c. distributions of PS and PI homopolymers in RI monitor; [PS]<sub>F</sub>, PS mole fraction in the feed mixture

heteroarm copolymers, anionic copolymerizations of binary macromonomers were carried out under similar polymerization conditions but on a larger scale. Separation of heteroarm copolymers was achieved by the following method. First, the copolymerization product was extracted by *n*-hexane to remove PI homopolymer. Next, the precipitation fractionation was carried out in the benzene-methanol system at 20°C in order to separate PS homopolymer; the turbidity of the copolymerization product was measured beforehand at a wavelength of 500 nm (Hitachi Perkin-Elmer 139 u.v.-vis. spectrometer).

#### Characterization of heteroarm star copolymers

The weight-average molecular weight ( $\bar{M}_w$ ) of heteroarm copolymers was determined by static light scattering (SLS) on a Photal SLS 700 (Otsuka Electronics Ltd) with a helium/neon laser. The scattering angles were in the range 30–150°. The index matching solvent was benzene. Samples were filtered through membrane filters with nominal pore size of 0.2  $\mu\text{m}$  before measurement. Solutions were measured in the concentration range 2–10  $\text{mg ml}^{-1}$  and the radii of gyration ( $R_g$ ) obtained by extrapolation to infinite dilution.

The composition of heteroarm copolymers was determined by  $^1\text{H}$  n.m.r. (90 MHz, JEOL FX-90Q n.m.r. spectrometer) in  $\text{CDCl}_3$ .

#### Morphological observation

Morphological observations were performed as follows. Heteroarm copolymer film (40  $\mu\text{m}$  thick) was cast from a 0.03  $\text{g ml}^{-1}$  benzene solution onto a Teflon sheet (0.11  $\text{ml cm}^{-2}$ ) as substrate. The casting solvent was evaporated as slowly as possible under saturated vapour. The films were annealed at 110°C for 2 days. Next, the films were embedded in an epoxy resin and cut, perpendicularly to the film interfaces, into ultrathin sections (700–1000 Å thick) using an ultramicrotome (Reichert-Nissei Co., Ultracut N). This specimen was exposed to osmium tetroxide ( $\text{OsO}_4$ ) vapour for 24 h.

Morphological results were obtained by transmission electron microscopy (TEM, Hitachi H-500 at 75 kV).

## RESULTS AND DISCUSSION

### Synthesis of vinylbenzyl-terminated macromonomers

Tables 1 and 2 list characteristics of vinylbenzyl-terminated PS and PI macromonomers, respectively. The conversion was almost 100% within experimental error in SM and IM macromonomers. The g.p.c. profiles showed that SM and IM macromonomers had a single and relatively narrow molecular weight distribution. The direct coupling of polystyryl anion with CMS formed the SM macromonomer possessing one vinylbenzyl group at the terminal end. In a previous article<sup>20</sup>, we reported that the direct coupling of poly(styrene-*b*-isoprene) diblock living anion with CMS caused the formation of some dimeric block copolymer by electron transfer. In the termination reaction of the IM series, the end of PI living anions was capped with MS units. As a result, the end-group functionality of IM macromonomers was determined to be unity by using g.p.c. calibration.

### Copolymerization reactivity

Anionic copolymerizations of binary SM and IM macromonomers were carried out in benzene, varying the feed molar ratio of SM( $M_1$ ) to IM( $M_2$ ) macromonomers (macromonomer concentration  $\sim 0.02 \text{ g ml}^{-1}$ ). Table 3 lists the copolymerization conditions and the composition of heteroarm copolymers ( $F_1$  and  $f_1$  indicate the  $M_1$  fraction of feed macromonomer concentration and the  $M_1$  fraction in the heteroarm copolymer, respectively). Typical g.p.c. profiles of HA1-1 and HA1-3 are shown in Figure 2. In both copolymerization series, new peaks appear at the high molecular weight side compared with SM and IM macromonomers. These peaks correspond to heteroarm copolymers. After separation of the distribution of heteroarm copolymer by simulation, using a personal computer,  $f_1$  was determined by the calibration curve shown in Figure 1.

Figure 3 shows the instantaneous composition (mole fraction  $f_1$ ) as a function of macromonomer composition (mole fraction  $F_1$ ) for the HA1 and HA2

**Table 3** Copolymerization conditions and composition of heteroarm copolymers<sup>a</sup>

No.	Feed macromonomer			Heteroarm copolymer, $f_1^e$
	$M_1^b$	$M_2^c$	$F_1^d$	
HA1-1			16.9	14.8
HA1-2			28.9	24.3
HA1-3	SM2	IM2	50.0	43.6
HA1-4			59.4	69.0
HA1-5			79.7	83.7
HA2-1			27.5	11.3
HA2-2	SM1	IM1	50.5	33.1
HA2-3			69.6	42.6
HA2-4			85.7	59.0

<sup>a</sup> Polymerized in benzene initiated by *n*-BuLi at 25°C (macromonomer concentration  $\sim 0.02 \text{ g ml}^{-1}$ )

<sup>b</sup> SM1,  $DP = 121$ ; SM2,  $DP = 274$

<sup>c</sup> IM1,  $DP = 283$ ; IM2,  $DP = 289$

<sup>d</sup>  $M_1$  mole fraction in feed macromonomers

<sup>e</sup>  $M_1$  mole fraction in heteroarm copolymers; determined by g.p.c. with r.i. and u.v. double detectors

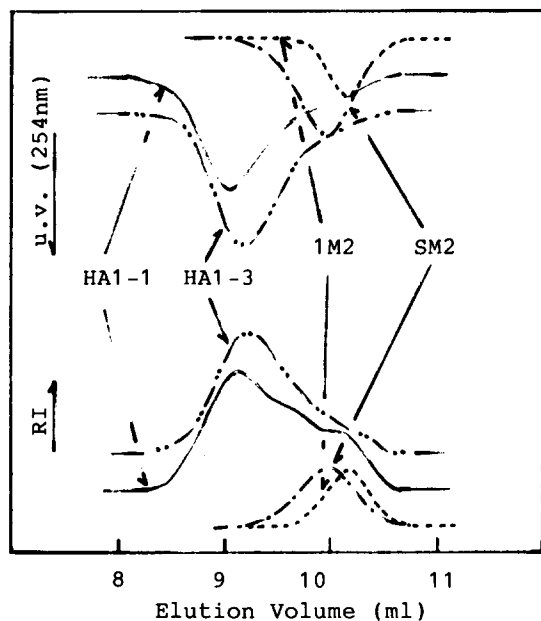
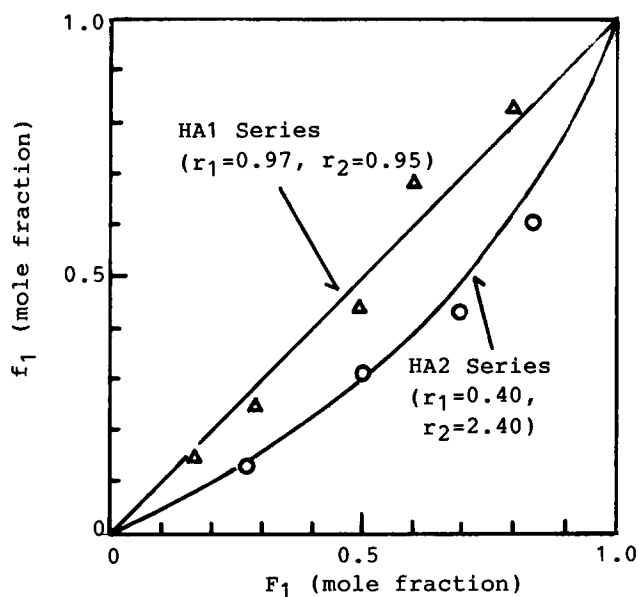


Figure 2 G.p.c. profiles of HA1 series and macromonomers


 Figure 3 Instantaneous composition (mole fraction  $f_1$ ) as a function of macromonomer composition (mole fraction  $F_1$ ) for HA1 and HA2 copolymerization series

copolymerization series. It is found from these curves that the HA1 series ( $r_1=0.97$  and  $r_2=0.95$ ) proceeds with azeotropic copolymerization. So, when  $r_1=r_2=1$ , the macromonomers show equal reactivity towards both propagating species, and the copolymer composition is the same as the comonomer composition. In this copolymerization system, the degree of polymerization ( $DP$ ) of both macromonomers was almost the same (for SM2  $DP=274$ , for IM2  $DP=289$ ). However, in the case of HA2, where the two reactivities are different ( $r_1=0.40$  and  $r_2=2.40$ ), the IM macromonomer is more reactive and the heteroarm copolymer contains a large proportion of the more reactive monomer in random placement. In the HA2 system, the  $DP$  of the IM macromonomer was larger than that of SM (for SM1  $DP=121$ , for IM1  $DP=283$ ).

The polymerization mechanism can be explained as follows. (1) In the HA2 system, micelles of core (PS segments)-corona (PI segments) type are formed during copolymerization. The IM macromonomers are compatibilized predominantly with these corona parts. Then the collision frequency of propagating anions on the domain interface with PI macromonomers increases compared to that with SM macromonomers. (2) In the HA1 system, the micelles formed may have a worm-like morphology because the macromonomers have the same  $DP$ . The probability of incorporating binary macromonomers in micelles is almost equal during copolymerization. Thus, the reactivity ratios seem to depend strongly on the morphology of micelles even in copolymerization systems of binary macromonomers composed of the same functional group.

#### Microphase separation of heteroarm copolymers

Anionic copolymerizations of SM2 and IM1 macromonomers were carried out in benzene (S1 and S2). A

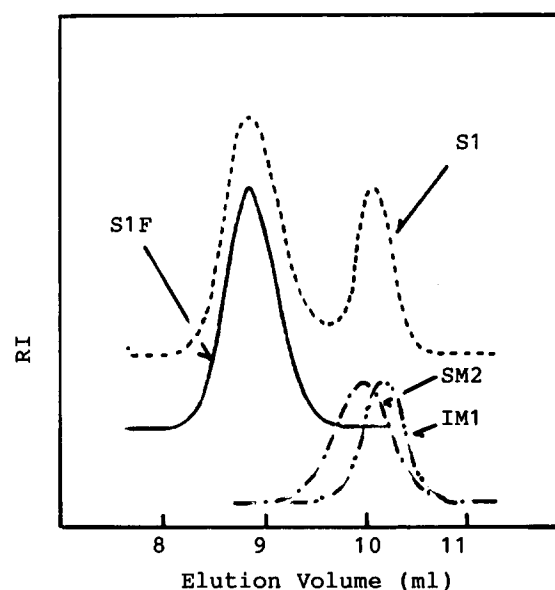


Figure 4 G.p.c. profiles of S1, S1F and macromonomers

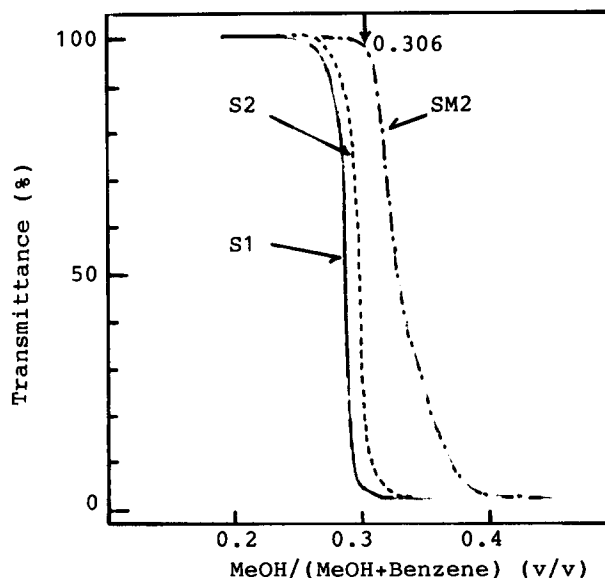


Figure 5 Turbidity curves of S1, S1F and SM2 macromonomer

typical g.p.c. profile of the copolymerization product removed, IM1 (S1), is shown in *Figure 4*. It is found from these results that the g.p.c. curve of S1 is bimodal. The first peak at lower elution volume is ascribed to the SM2 macromonomer. The second peak at higher elution volume corresponds to the heteroarm copolymer. The g.p.c. profile also shows that this heteroarm copolymer has a narrow molecular weight distribution.

In order to separate the unreacted SM2 from the copolymerization product, precipitation fractionations

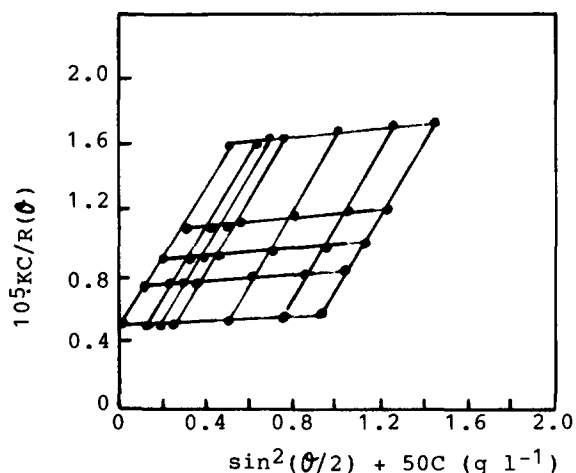


Figure 6 Zimm plot of heteroarm copolymer S1F

were carried out in a benzene-methanol (precipitant) system. Typical turbidity curves of the copolymerization series (S1 and S2) are shown in *Figure 5*. It is found from these curves that the SM2 macromonomer is precipitated at a precipitant fraction value of 0.306 (indicated by an arrow). A typical g.p.c. profile of fraction S1F is shown in *Figure 4*. The g.p.c. profile shows that fraction S1F has a single molecular weight distribution. *Figure 6* shows a typical Zimm plot of S1F obtained by means of SLS. The  $\bar{M}_w$  and  $R_g$  values were determined from this plot. *Table 4* lists the characteristics of heteroarm copolymers. The composition of heteroarm copolymers obtained in this work is in the range of 61–66 mol% PS blocks. The molecular weight distribution of both copolymer samples is very narrow ( $\bar{M}_w/\bar{M}_n = 1.07$ ).

Typical TEM micrographs of specimen S1F are shown in *Figure 7*. The heteroarm star copolymer forms a clear microphase-separated structure. More recently, Takano *et al.*<sup>24</sup> have prepared heteroarm star copolymers by the coupling of PS and PI living anions with 4-vinylphenyl dimethylvinylsilane. They could not detect a microphase-separated structure for the heteroarm star copolymer prepared. This type of  $A_nB_n$  star copolymer is constructed by bringing  $n$  identical diblock copolymers together and joining them at their A–B junction points. Takano *et al.*<sup>24</sup> explained their result (i.e. no microphase separation) by suggesting that A and B arms are in equilibrium with each other owing to the effect of the junction constraint. However, there are two entropic effects at work here that oppose one another, according to de la Cruz and

Table 4 Characteristics of heteroarm star copolymers and domain sizes

Code	$\bar{M}_w^a \times 10^{-5}$	$\bar{M}_w/\bar{M}_n^b$	$R_g^c \times 10^{-2}$ (Å)	PS arm <sup>d</sup> (mol%)	Arm number <sup>e</sup>		Domain size, $R^f$ (nm)
					PS	PI	
S1F	2.01	1.07	2.38	66.2	4.8(4.0)	2.5(3.7)	12.1
S2F	1.61	1.07	3.26	61.4	3.7(3.4)	2.1(2.6)	12.0

<sup>a</sup> Determined by Zimm plot

<sup>b</sup> Determined by g.p.c.

<sup>c</sup> Radius of gyration, determined by SLS

<sup>d</sup> Determined by <sup>1</sup>H n.m.r.

<sup>e</sup> Determined by the relation of composition (<sup>1</sup>H n.m.r.) and  $M_w$ . Values in parentheses indicate arm numbers determined by the relation of composition (g.p.c. calibration) and  $M_w$

<sup>f</sup> Radius of PI cylinders, determined by TEM micrographs

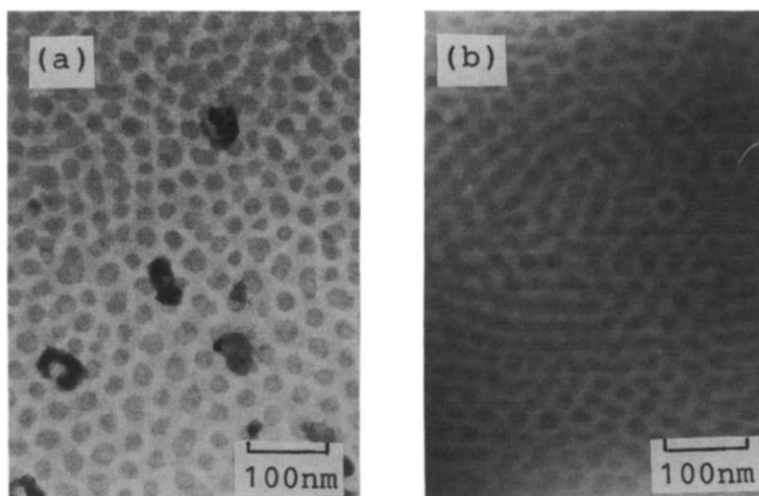


Figure 7 TEM micrographs of heteroarm copolymer S1F specimen cast from benzene

Sanchez's theory<sup>2</sup>. The first is the entropy of the melt. The entropy of the star copolymer is smaller than that of the corresponding diblock copolymer melt because of the additional constraints on the A-B junction point. However, for non-critical compositions, there will be a lowering of the transition entropy caused by the junction constraint. As a result, it is easier to phase-separate star copolymers than the corresponding diblock copolymers. It is very interesting to obtain clear microphase separation of heteroarm copolymers in this investigation. From the TEM micrograph (Figure 7a) it is seen that PI microdomains form an ordered hexagonal arrangement in a two-dimensional aspect. Moreover, a morphology of PI cylinders appears in another part of specimen S1F (Figure 7b). So, it can be judged from these results that the equilibrium morphology of specimen S1F is of dispersed PI cylinders in a PS matrix. The TEM micrographs of specimen S2F indicated the same morphology. The average radii ( $\bar{R}$ ) of PI cylinders for S1F and S2F specimens are listed in Table 4.

In diblock copolymers exhibiting cylindrical microdomains, the 2/3 power law is consistent with the results

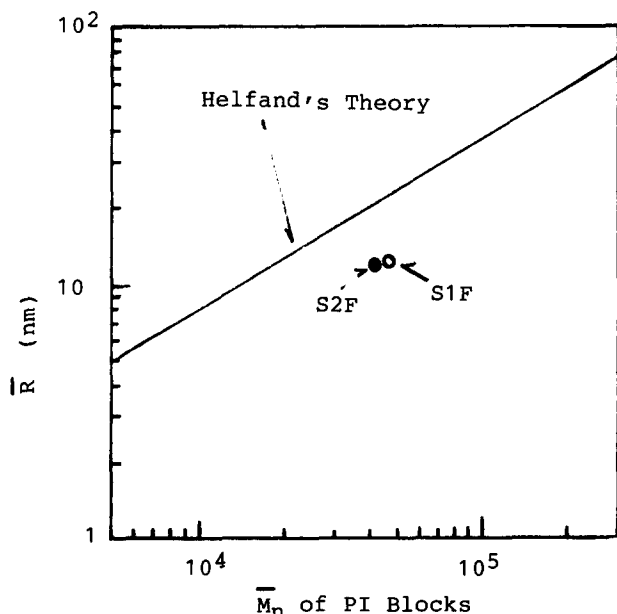


Figure 8 Plot of the average cylinder radius  $\bar{R}$  versus the molecular weight  $\bar{M}_n$  of the PI blocks for heteroarm copolymers and diblock copolymers

predicted from the equilibrium theory of Helfand and Wasserman<sup>25</sup>. We compared the domain spacing of heteroarm copolymers (S1F and S2F) with that of corresponding diblock copolymers (Figure 8). It is found from these plots that the absolute values of PI cylinders for heteroarm copolymers are below the theoretical line for diblock copolymers. The mechanism of such microphase separations may be explained as follows. Matsushita *et al.*<sup>26</sup> have studied the chain conformation and location of parts of a diblock copolymer in a lamellar structure by small-angle neutron scattering. They clearly showed that the chain adjacent to the junction between the two blocks was located near the boundary between domains and was contracted along the direction parallel to the lamellae to the same extent as a whole block chain with the same molecular weight, while the chain at the free end of the block copolymer was located in the middle of the domain and was unperturbed. A schematic drawing of such chain conformations of block chains is shown in Figure 9a, where  $A_B$  and  $B_B$  indicate the volume of A and B blocks, respectively, and  $(D_B)_B$  is the domain size of polyB phases. Figure 9b shows the predictable chain conformations of arm chains for heteroarm star copolymer.  $B_H$  ( $A_H$ ) is the volume of B (A) arms and is equal to  $B_B$  ( $A_H$ ) owing to the same molecular weight. However, it can be expected that A and B arms are not contracted along the direction parallel to the interface owing to the effect of the junction constraint. As a result, the domain size of polyB phases for heteroarm copolymer  $(D_B)_H$  seems to be smaller than  $(D_B)_B$ . The chain conformations in cylindrical microdomains probably take the same arrangement as those in lamellar microdomains. The above speculation still holds, although quantitative experiments are necessary.

## REFERENCES

- 1 Leibler, L. *Macromolecules* 1980, **13**, 1602
- 2 de la Cruz, M. O. and Sanchez, I. C. *Macromolecules* 1986, **19**, 2501
- 3 Berlinova, I. V. and Panayotov, I. M. *Makromol. Chem.* 1989, **190**, 1515
- 4 Tsitsilianis, C., Chaumont, P. and Rempp, P. *Makromol. Chem.* 1990, **191**, 2319
- 5 Tsitsilianis, C., Graff, S. and Rempp, P. *Eur. Polym. J.* 1991, **27**, 243
- 6 Penisi, R. W. and Fetters, L. J. *Macromolecules* 1988, **31**, 1094
- 7 Quirk, R. P., Lee, B. and Schock, L. *Makromol. Chem. Macromol. Symp.* 1992, **53**, 201
- 8 Quirk, R. P. and Ingatz-Hoover, F. in 'Recent Advances in

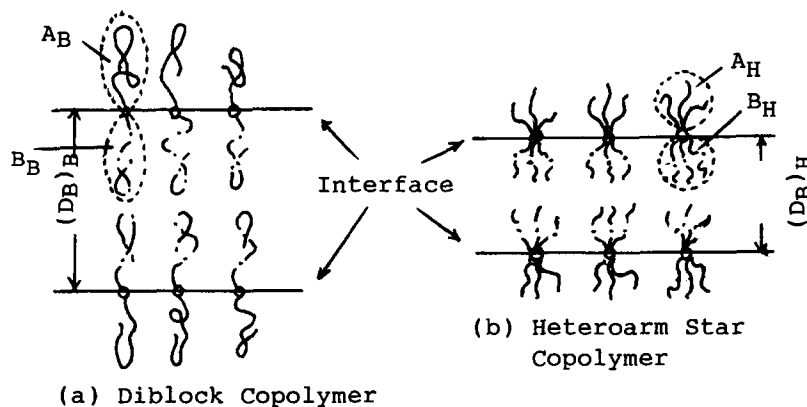


Figure 9 Schematic drawing of the chain conformations of block chains for (a) diblock copolymer and (b) heteroarm star copolymer

- Anionic Polymerization' (Eds T. E. Hogen-Esch and J. Smid), Elsevier, New York, 1987, p. 393
- 9 Einert, G. and Herz, J. *Makromol. Chem.* 1980, **181**, 59
- 10 Eshwey, H. and Burchard, W. *Polymer* 1975, **16**, 180
- 11 Kanaoka, S., Omura, T., Sawamoto, M. and Higashimura, T. *Macromolecules* 1992, **25**, 6407
- 12 Hashimoto, T., Shibayama, M. and Kawai, H. *Macromolecules* 1980, **13**, 1237
- 13 Shibayama, M. and Hashimoto, T. *Macromolecules* 1986, **19**, 740
- 14 Tanaka, H. and Nishi, T. *J. Chem. Phys.* 1986, **82**, 4326
- 15 Anastasiadis, S. H., Russell, T. P., Satija, S. K. and Majkrzak, C. F. *Phys. Rev. Lett.* 1989, **62**, 1852
- 16 Ishizu, K., Yukimasa, S. and Saito, R. *Polymer* 1992, **33**, 1982
- 17 Ishizu, K., Yukimasa, S. and Saito, R. *Polym. Commun.* 1991, **32**, 386
- 18 Ishizu, K. and Kuwahara, K. *J. Polym. Sci., Polym. Chem. Edn* 1993, **31**, 661
- 19 Asami, R., Takaki, M. and Hatanaka, H. *Macromolecules* 1983, **16**, 268
- 20 Ishizu, K., Shimomura, K. and Fukutomi, T. *J. Polym. Sci., Polym. Chem. Edn* 1991, **29**, 923
- 21 Pierce, P. E. and Armonas, J. E. *J. Polym. Sci.* 1968, **C21**, 23
- 22 Mayo, F. R. and Lewis, F. M. *J. Am. Chem. Soc.* 1944, **66**, 1594
- 23 Fineman, M. and Ross, S. D. *J. Polym. Sci.* 1950, **5**, 269
- 24 Takano, A., Ozawa, H., Kazama, T. and Isono, Y. *Polym. Prepr. Jpn* 1992, **41(9)**, 3786
- 25 Helfand, E. and Wasserman, Z. R. *Macromolecules* 1980, **13**, 994
- 26 Matsushita, Y., Mori, K., Mogi, Y., Saguchi, R., Noda, I., Nagasawa, M., Chang, T., Glinka, C. J. and Han, C. C. *Macromolecules* 1990, **23**, 4387